SCIENCE CHINA
Earth Sciences

SPECIAL TOPIC: China since the Last Glacial Maximum
•RESEARCH PAPER•

August 2019 Vol.62 No.8: 1302–1315
https://doi.org/10.1007/s11430-018-9304-y

Holocene aeolian stratigraphic sequences in the eastern portion of the desert belt (sand seas and sandy lands) in northern China and their palaeoenvironmental implications

Xiaoping YANG[1*], Peng LIANG[2,3], Deguo ZHANG[1], Hongwei LI[1], Patrick RIOUAL[2], Xulong WANG[4], Bing XU[2], Zhibang MA[2], Qianqian LIU[5], Xiaozong REN[6], Fangen HU[7], Yuxin HE[8], Gang RAO[8] & Ninghua CHEN[8]

[1] *Department of Geography, School of Earth Sciences, Zhejiang University, Hangzhou 310027, China;*
[2] *Key Laboratory of Cenozoic Geology and Environment, Institute of Geology and Geophysics, Chinese Academy of Sciences, Beijing 100029, China;*
[3] *University of Chinese Academy of Sciences, Beijing 100049, China;*
[4] *State Key Laboratory of Loess and Quaternary Geology, Institute of Earth Environment, Chinese Academy of Sciences, Xi'an 710061, China;*
[5] *Institute of Chinese Historical Geography, Fudan University, Shanghai 200433, China;*
[6] *School of Geography, Taiyuan Normal University, Taiyuan 030619, China;*
[7] *College of Teachers' Education, Yichun University, Yichun 336000, China;*
[8] *Department of Geology, School of Earth Sciences, Zhejiang University, Hangzhou 310027, China*

Received March 12, 2018; revised October 22, 2018; accepted November 9, 2018; published online February 22, 2019

Abstract This paper presents the environmental history and its responses to palaeoclimatic changes since the start of the Holocene in the eastern portion of the desert belt (sand seas and sandy lands) in northern China by comparing the aeolian sand-palaeosol sequences and their palaeoclimatic proxies. The optically stimulated luminescence (OSL) ages of the aeolian sand-palaeosol sedimentary sequences and a series of palaeoenvironmental proxies show that: (1) The large-scale dune landscape currently in the Kubuqi Sand Sea was formed during the Holocene in general; and the palaeosol was generally developed during the period of 4–2 ka, indicating conditions favorable for vegetation growth, soil development, and organic carbon accumulation due to increased precipitation or effective moisture and weakened aeolian activities; the large-scale expansion of dunes in the recent 2 ka is closely linked to human activities. The variable discharge of the Yellow River with diversions for irrigation may have resulted in a more consistent supply of aeolian particles for dune field expansion. (2) The dune landscape of the Hunshandake Sandy Land was likely formed around 12 ka, and before this, the western part of the Hunshandake Sandy Land would have been covered by a single large lake; it was obviously wetter than today in the sandy land during the period of 9.6–3 ka and the palaeosols were developed at the same time. But the aeolian activities have not been completely dormant in this long-lasting wetter epoch; because the Holocene wetter period was likely time-transgressive across the region. (3) The palaeosol of the Hulunbuir Sandy Land began to develop as early as 14.5 ka, probably continuing until the last 2 ka. The palaeosol development of various dune fields in the eastern portion of the desert belt (sand seas and sandy lands) in northern China is spatially heterogeneous, and even the palaeosol development time in different locations within each sandy land is inconsistent. During the middle Holocene (especially the 7.5–3.5 ka), all the sandy lands were stabilized in general and the intensity of aeolian activities was significantly weakened. The number of palaeoenvironmental records in the eastern portion of the desert belt (sand seas and sandy lands) in northern China has increased rapidly in the past decade, but the amount of published data still does not match the vast extent of the dune fields. It does require much more in-depth palaeoenvironmental studies for a full understanding of the relationship between aeolian activities and climate change in northern China.

* Corresponding author (email: xpyang@zju.edu.cn)

Keywords Sand sea; Sandy land, Environmental evolution, Kubuqi, Hunshandake, Hulunbuir

Citation: Yang X, Liang P, Zhang D, Li H, Rioual P, Wang X, Xu B, Ma Z, Liu Q, Ren X, Hu F, He Y, Rao G, Chen N. 2019. Holocene aeolian stratigraphic sequences in the eastern portion of the desert belt (sand seas and sandy lands) in northern China and their palaeoenvironmental implications. Science China Earth Sciences, 62: 1302–1315, https://doi.org/10.1007/s11430-018-9304-y

1. Introduction

Sand Seas and Sandy Lands, which occupy 6% of the global land surface, are common landscapes in drylands of Earth (Pye and Tsoar, 2009). The deposits of aeolian sand and their stratigraphic sequences, which record the environmental changes of the dune fields and their responses to the global climate changes as well as human activities, are unique and important sedimentary and geomorphic archives of dryland evolution (Goudie, 2002; Lancaster et al., 2013, 2016; Williams, 2014). In China, about 566000 km^2 of landmass are covered by wind-blown sands. The Sand Sea landscape dominated by active sand dunes is mainly distributed in the arid regions with a mean annual precipitation less than 200 mm, while the Sandy Land landscape dominated by semi-active and vegetated dunes mainly occur in the semi-arid regions with a mean annual precipitation of 200–400 mm (Zhu et al., 1980).

In recent years, scientific issues such as greenhouse gas emissions, which should have a causal relation to global warming and the increase of extreme climate events, have attracted widespread attention from scientific communities and policymakers in various countries (IPCC, 2013). One of the key tasks of the Strategic Priority Project "Carbon Budgets and Related Issues" granted by the Chinese Academy of Sciences has been to assess the palaeoenvironmental patterns of China and the responses of ecosystems to climate change during the typical geological time windows, and to provide "historical analogue" for human adaptations to climate changes in the future (Guo et al., 2016). Numerical simulations indicate that under the background of increased CO_2 emissions and global warming, the global dryland area would expand rapidly and experience enhanced land degradation (Cherlet et al., 2018). Under the RCP8.5 scenario, the global dryland would increase to 56% of the land surface at the end of this century (Dai, 2013; Huang et al., 2016). As a predominant landscape of drylands, how does the sand dune system respond to climate change is an urgent and challenging environmental issue that human society has to face (Cherlet et al., 2018). Additionally, studies have shown that the desert ecosystem is the third largest active carbon pool on landmass outside of terrestrial plants and soils, and it plays a key role in regulating the concentration of atmospheric CO_2 and global climate change (Wohlfahrt et al., 2008; Stone, 2008; Evans et al., 2014; Li et al., 2015; Liu et al., 2015). In order to understand the response mode of dune fields to climate change, it is important to study the temporal and spatial variation characteristics of dune systems in the recent past and their reactions to different palaeoclimates comprehensively on the basis of the palaeoenvironmental record from the interior of the dune fields.

Compared with other deserts of the world, the number of palaeoenvironmental records from Chinese deserts is much smaller. It was hampered by the low accessibility of Sand Seas, and the lack of reliable and high precision dating methods in the past, as well as the high complexity and vast distribution of the dunes in China. Early research regarding the formation history of deserts was mainly focused on the margins of the Sand Seas or Sandy Lands and induced the past environmental changes from some indirect archives such as loess deposits adjacent to the deserts (Zhu et al., 1980), with just a very limited direct records from the interior of dune fields. With the rapid development of luminescence dating in recent decades, which provides the possibility to date the aeolian events directly, the number of palaeoenvironmental records from internal deserts has increased accordingly (e.g., Yang et al., 2003, 2006, 2013, 2015; Lu et al., 2005, 2013; Zhou et al., 2008; Mason et al., 2009; Stauch et al., 2012; Gong et al., 2013; Fan et al., 2013; Qiang et al., 2016; Stauch, 2016; Yang et al., 2017; Guo et al., 2018). The records from internal deserts with their physical dating data provided some direct information and evidence of the processes and mechanisms of the desert formation and landscape evolution. As of now, more than 300 age records from the dune fields of north China have been published, and most of them derived from the sandy lands in the eastern portion of the desert belt in northern China (Li and Yang, 2016). Several studies demonstrated that the sandy lands of eastern China have experienced significant environmental changes since the Last Glacial Maximum (LGM), and most of the dunes in the sandy lands have been vegetated extensively during the middle Holocene (Zhu et al., 1988; Lu et al., 2005; Mason et al., 2009; Yang et al., 2013). For example, there were frequent aeolian activities in the Maowusu Sandy Land during the early Holocene (11.5–8 ka), but the aeolian sands were gradually stabilized after 8 ka as the monsoon weakened and lower temperatures reduced evapotranspiration (Mason et al., 2009). A study from Hunshandake Sandy Land demonstrated that most of the dunes were stabilized by vegetation during 9.6–3 ka, but a few active dunes persisted in the west portion of the Sandy Land during the wetter epoch too (Yang et al., 2013). Studies from the Horqin Sandy

Land indicated that active dunes existed extensively before ~10 ka, and they were basically fixed during 8–3 ka, but some of them underwent several epochs of reworking and re-stabilizing after 3 ka (Zhao et al., 2007; Yang et al., 2010, 2012). These studies tried to reconstruct the history of environmental changes in the Sandy Lands through some individual aeolian depositional sequences, but the spatial heterogeneity within the Sandy Lands makes the representativeness of these individual sedimentary sections questionable (Liang and Yang, 2016).

With the strong support of the research programme "Environmental Pattern of China during the Holocene Thermal Maximum", one of a subproject of the Strategic Priority Project "Carbon Budgets and Related Issues", we conducted studies on the Sand Seas and Sandy Lands in the eastern portion of Chinese desert belt (Figure 1). In this paper, we mainly review the recent endeavors in the studies of the chronology, geomorphology, and palaeoclimatology of dune systems, especially the typical Holocene aeolian stratigraphic sequences from Kubuqi, Hunshandake, and Hulunbuir. The main aim of this paper is to examine the landscape evolution history and their spatial and temporal variations in the dune fields in eastern China during the Holocene. The palaeoclimatic implications of the aeolian records will also be discussed.

2. Regional settings

East of the Helan Mountains (~106°E) the deserts consist mainly in Sandy Lands except for the Kubuqi Sand Sea, the only one dominated by active dunes. The dune fields (including Sand Seas and Sandy Lands) in the eastern part of the desert belt in northern China are Kubuqi Sand Sea, Maowusu Sandy Land, Hunshandake Sandy Land, Hulunbuir Sandy Land and Horqin Sandy Land, respectively (Zhu et al., 1980; Figure 1). While the palaeoenvironmental records in the western portion of the Chinese desert belt are mainly represented by calcareous cementation layers and lacustrine deposits (Yang, 2000; Zhang et al., 2002; Chen et al., 2003; Yang et al., 2003, 2006, 2011), the Sandy Lands in the east show a distinct alternation of buried soil and aeolian sands, indicating vegetation growth and aeolian activities, respectively (Lu et al., 2005; Mason et al., 2009; Yang et al., 2011, 2013; Guo et al., 2018).

The Kubuqi Sand Sea located on the northern Ordos Plateau and the southern bank of the Yellow River (Figure 1), extends ~300 km from west to east, and its width decreases from ~100 km in the west to 20–30 km in the east. Ten tributaries (perennial and seasonal) of the Yellow River with headwaters in the northern Ordos Plateau flow through the middle and eastern part of Kubuqi northward. The Kubuqi Sand Sea lies on the margin of the East Asian Summer Monsoon, and the mean annual precipitation decreases from ca. 400 mm in the east to 150 mm in the west (Figure 1). Despite a relatively high mean annual precipitation, 80% of the dunes in the Kubuqi are active (Zhu et al., 1980). Therefore, it is the only sand sea in the semi-arid areas of China. Tall transverse dunes overlie the fluvial-alluvial terraces of the Yellow River's tributaries and the strikes of these dunes are perpendicular to the predominant WWN winds (Yang et al., 2016).

The Hunshandake Sandy Land is in the eastern Inner Mongolia (Figure 1). Due to the reducing influence of the East Asian Summer Monsoon, the mean annual precipitation decreases from ca. 450 mm in the southeast to 150 mm in the northwest (Yang et al., 2013; Figure 1). The landscapes are dominated by active dunes and semi-stabilized dunes, such as barchan and barchan chains (up to 10 m), in the western part, while the eastern part is covered by a relatively dense vegetation, and dunes are generally stabilized by plants. Most of dunes in the east show parabolic, linear and network forms (Zhu et al., 1980; Yang et al., 2008).

The Hulunbuir Sandy Land is at the highest latitudes, compared to other aeolian landscapes in China (Figure 1). The mean annual precipitation decreases from ca. 350 mm in the east to 280 mm in the west (Figure 1), and the mean annual temperature is about −1°C. Several rivers with headwaters in the Greater Higgnan Mountains bring enough sands to the Hulunbuir Sandy Land. In general, the Hulunbuir Sandy Land has a high vegetation coverage, reaching up to 30% and even to 50% on dune surfaces. The Hulunbuir Sandy Land consists of three separate sandy belts from north to south: the north one is located on the southern bank of the Hailar river, with a length of about 110 km from east to west, and active dunes, blowouts, and semi-stabilized dunes are common; the central belt is characterized with stabilized parabolic and re-activated dunes, with a height of about 5–15 m; the dunes in the south belt are stabilized, with scattered blowouts (Zhu et al., 1980).

3. Materials and methods

During field investigations, we selected 7 typical aeolian sand-palaeosol sections in the Kubuqi Sand Sea, the Hunshandake Sandy Land and the Hulunbuir Sandy Land (Figure 1). Detailed interpretation of sedimentary facies was carried out according to the stratigraphic features, such as colour, particle size, bedding, texture and sedimentary structure in the field, and chronological and proxies' samples were collected at locations with palaeoenvironmental significance. The chronological framework of the sedimentary sections was established by OSL dating. In addition to the interpretation of sedimentary facies in the field, grain size and magnetic susceptibility were measured in laboratories.

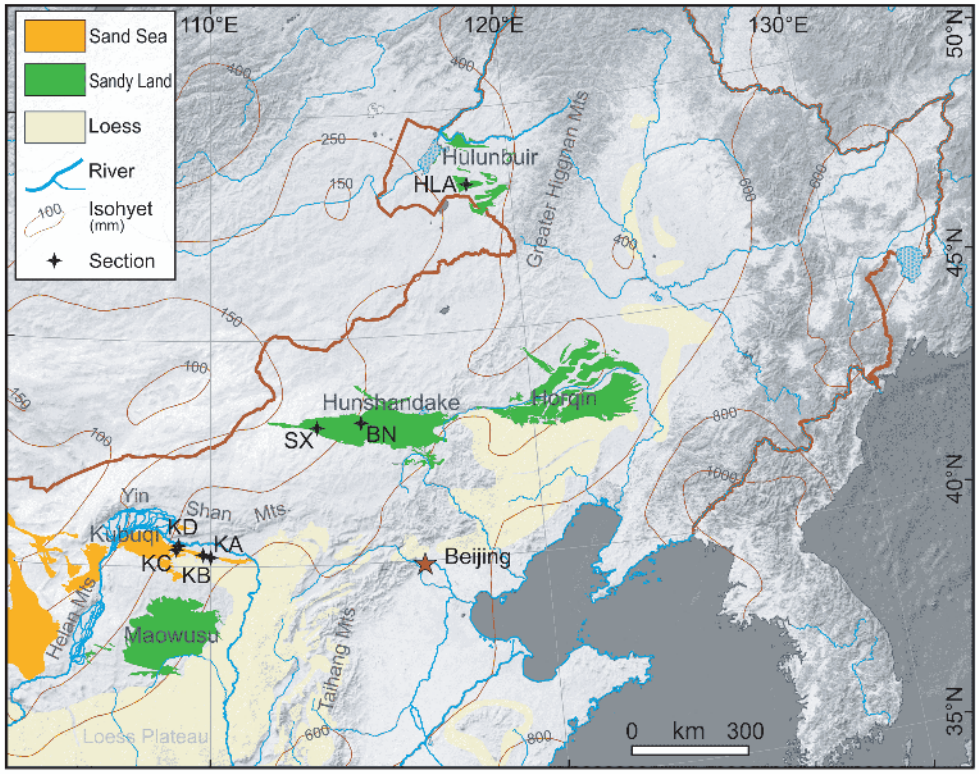

Figure 1 Distribution of dune fields in the eastern portion of the Chinese desert belt and the locations of sections (The boundary of the dune fields mapped by the authors from Google Earth imagery. The precipitation data is from WorldClim (v2.0) dataset (Fick and Hijmans, 2017).

In this paper, OSL data of the six sections collected from the Kubuqi Sand Sea and the Hunshandake Sandy Land are sourced from Yang et al. (2013, 2016). Chronological samples of HLA from the Hulunbuir Sandy Land were dated in the Laboratory of OSL Chronology, Institute of Earth Environment, Chinese Academy of Sciences (CAS) in Xi'an, and equivalent dose (De) measurements were performed on an automated Daybreak 2200 system following the Single Aliquot Regeneration (SAR) protocols (Murray and Wintle, 2000, 2003). The environmental dose rate was calculated according to the content of U, Th, and K of each sample (Guérin et al., 2011). Water content and cosmic dose rate also were considered.

The grain size of samples from the Hulunbuir Sandy Land was determined with a Malvern Mastersizer 3000. The mean grain size (Mz) and standard deviation (σ) were calculated following Folk and Ward (1957). Magnetic susceptibility was measured with a Bartington MS2 susceptibility meter, measurements involved dual frequencies of 465 Hz (low frequency, χ_{lf}) and 4650 Hz (high frequency, χ_{hf}), and the percentage frequency-dependent susceptibility (χ_{fd}, %) was calculated with the following formula: $\chi_{fd}=[(\chi_{lf}-\chi_{hf})/\chi_{lf}]\times100\%$ (Heller et al., 1991). All above measurements were taken in the Key Laboratory of Cenozoic Geology and Environment, Institute of Geology and Geophysics, Chinese Academy of Sciences.

4. Results

4.1 Kubuqi Sand Sea

Section KA (40°14′N, 109°57′E) is exposed at 100 m above a tributary of the Yellow River. The entire section is 4.4 m thick, containing two layers of aeolian sands on the top and at the bottom of the sequence and an interbedded palaeosol (Figure 2). The bottom aeolian sand unit can be divided into two parts: the lower part (4.4–4 m) is moderately sorted, light yellowish brown (10YR 6/4), fine sand. The upper part (4–3.4 m) is moderately well sorted, yellowish brown (10YR 6/6), fine to medium sand, and has coarser grain size composition as well as lower contents of $CaCO_3$, TC, and magnetic susceptibility compared with the lower part (Figure 2). The palaeosol (from 3.4 to 1.5 m) is poorly sorted, brown (10YR 5/3), silty fine to fine sand. The upper 10 cm of the palaeosol is a culture layer, composed of moderately sorted, silty fine sand with some black carbon bits (Figure 2). Compared with the aeolian sands on the bottom, the palaeosol is much finer and more poorly sorted (Figure 2). The palaeosol is chronologically constrained by three OSL ages, i.e., 3850±440 yr at the base, 1900±195 yr in the middle and 905±12 yr on the top (Figure 2), indicating the palaeosol was developed during the period of ~4000 yr to 1000 yr. The uppermost layer of the section is 1.5 m thick, moderately well sorted, light yellowish brown (10YR 6/4), fine aeolian

sand, with well-developed cross beddings (Figure 2). Quartz grains from 1 m of this layer yielded an OSL age of 235±35 yr (Figure 2).

Section KB (40°17′N, 109°47′E) is a 3.2 m thick aeolian sand-palaeosol sequence exposed also on a terrace of a tributary of the Yellow River, 20 m above the present river channel. Two distinct aeolian sand layers are separated by a buried soil, same as the KA section. The basal unit of the section (3.2–2.4 m) is yellowish brown (10YR 6/4), moderately well sorted, fine sand. The OSL sample collected at 2.9 m yielded an age of 7870±745 yr (Figure 2). The palaeosol (2.4–0.35 m) is dark grayish brown (10YR 4/2), poorly sorted, silty sand. The upper 0.4 m of the palaeosol is differentiated by a weakly developed soil composed of brown (10YR 5/3), better sorted but coarser sand (Figure 2) with a weak blocky structure. The OSL ages indicate that the palaeosol horizons were formed between 2870±320 yr and 2175±290 yr. The buried soil is overlaid by a 0.4 m thick layer with light yellowish brown (10YR 6/4), very well sorted, fine to medium aeolian sands (Figure 2).

Section KC (40°22′N, 108°55′E) is located on the top of the first terrace of the Maobulakongdui, the largest river flowing through the Kubuqi Sand Sea, and this site is 22 m above the current river bed. The entire sequence is 3.7 m in thickness. The bottom unit (3.7–0.7 m) is light yellowish brown (10YR 6/4), well sorted, fine aeolian sand (Figure 2). The fluvial sediment of the upper unit (0.7–0 m) is light brown (7.5 YR 6/3), poorly sorted, clayey silt (Figure 2) with high content of $CaCO_3$ (up to 15%, Yang et al., 2006). Two hard calcareous cementation layers were identified around 0.6 m of the section, with a thickness of 2 cm, consisting mainly of white (5YR 8/1), silty sand and $CaCO_3$. This layer represents the latest flood event when the flooding level reached that height. The OSL ages indicate that the riverbed was in a quasi-stable state from 7520±590 to 3875±460 yr, and the aeolian deposition might occur near the river channel. The rapid alternating of aeolian sand and floodplain deposits on top of the section suggests that the river may have experienced multiple lateral swings after 3875±460 yr, thus forming intercalations of fluvial deposits and aeolian sands (Figure 2).

The oldest aeolian deposit that we have dated is at the bottom of KD section (40°24′N, 108°59′E; Figure 1), a sequence featured by aeolian sands with subhorizontal beddings. The sediments are white (5YR 8/1), poorly sorted, medium sands, with a high degree of carbonate cementation, and contain some subrounded gravels with a diameter of 2–3 mm. Quartz grains of aeolian sands were OSL dated to 16240±1410 yr. This sequence is exposed near the main channel of the Yellow River and was cut by fluvial incision of a tributary. From the sedimentary characteristics and the location, we think that this site was originally a part of an early channel of the tributary, and the aeolian sands belong to a type of source-bordering dunes.

Three of the four sections are not older than the Holocene, whereas the section KD having the oldest aeolian sand of the Kubuqi Sand Sea should be parts of a source-bordering dune. The palaeoenvironmental proxies, such as grain size, sorting (σ), $CaCO_3$, χ_{lf}, χ_{fd}, total carbon (TC), and total organic carbon (TOC), are quite different between aeolian sands and palaeosols (Yang et al., 2016).

4.2 Hunshandake Sandy Land

We conducted detailed fieldwork in the central and western parts of the Hunshandake Sandy Land, and two typical sections in the western Hunshandake were selected. Dense vegetation coverage around these two sections protects these regions from wind erosion at modern times. Section SX (43°04′N, 113°31′E) is located in a large interdune area, while section BN (43°08′N, 114°29′E) is on the western slope of a great lake basin surrounded by stabilized dunes. Most parts of the lake basin have dried up, and only a small shallow lake remains nowadays. The section BN is about 20 m above the current lake level.

On the basis of field observation, the section SX is divided into three units due to variations in colour, grain size, bedding and carbonate content (Figure 2). The upper unit (0.8–0 m) and basal unit (3.1–2 m) are light yellow (4–9Y 7–9/6–8) and white-yellow (0–3.5Y 8–9/4–8) aeolian sands, separated by a dark (9.5–9.7YR 5–7/4–8) palaeosol in the middle. Five OSL ages were initially obtained from the bottom of the section and the transitional zones of different units. Aeolian sand at the very bottom was dated to 12–13 ka. Though age inversion occurs between the two lowest samples (Figure 2), we still assume that the aeolian sand at the bottom of the section was about 13 ka, considering the error bars and uncertainties of the OSL ages. It also might indicate that aeolian sand at bottom of the section has a high accumulation rate. The development of palaeosol began at ca. 9.5 ±0.45 ka and ended at ca. 4.0±0.18 ka (Figure 2). According to the OSL ages, the mean sedimentation rate of the palaeosol was 12–15 cm kyr^{-1}, much lower than that of aeolian sands (30–75 cm kyr^{-1}).

The section BN shows similar sedimentary facies to those of the section SX, with a middle layer of palaeosol separating two aeolian sand units (Figure 2). The difference is that there is a 0.5 m thick fluvial and lacustrine sediment unit underlying the basal aeolian sands in the section BN. The upper 0.4 m of the fluvial and lacustrine unit is dark yellow (9YR 7/6), poorly sorted, coarse sand, quite different from aeolian sand, suggesting that it was probably a lakeshore while a great lake existed. The lower 0.1 m of the fluvial and lacustrine unit is well-consolidated silt and clay (Figure 2). The development of black-brown (6–7YR 2–2/2–7) palaeosol in the middle of the section BN began at 10.1±0.45 ka and

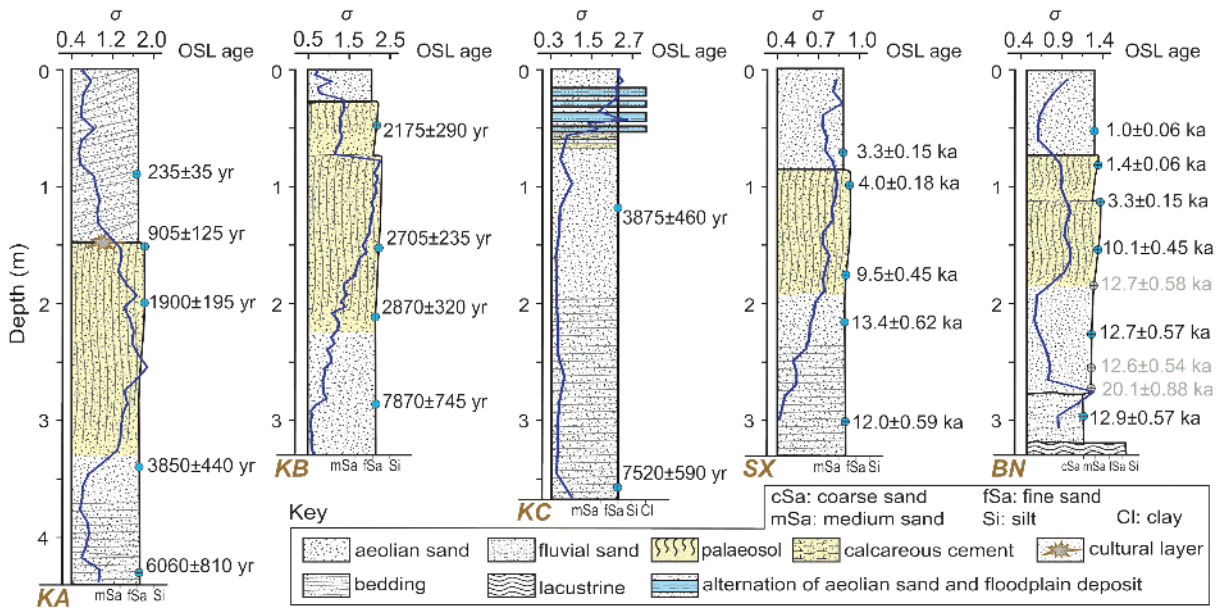

Figure 2 Stratigraphic sections with associated OSL ages and sorting (σ) of grain sizes (blue curve) from the Kubuqi Sand Sea (KA, KB and KC) and the Hunshandake Sandy Land (SX, BN) (for locations see Figure 1).

lasted until 3.3±0.15 ka. Besides, there is a transitional weak palaeosol horizon between the palaeosol and the uppermost aeolian sand unit, indicating a gradual enhancement of aeolian activities and degradation of vegetation. Aeolian sand samples from the upper and basal units were OSL dated to 1 ka and 13 ka, respectively. Considering the consistency of the whole chronology framework, we do not think the OSL age of the sample from the second lowest location (Figure 2) is reliable and thus it is not considered for further interpretation.

4.3 Hulunbuir Sandy Land

Section HLA (48°19′N, 118°58′E) is located on the eastern part of the central sand belt of the Hulunbuir Sandy Land (Figure 1), about 40 m above the current riverbed of the Hui River. The entire section is 3.5 m thick, and contains two palaeosol units (Figure 3). The bottom unit of the section (3.5–2.9 m) is well sorted, light brown (10YR 8/2.5), aeolian sand with near-horizontal bedding. Overlying is a 0.45 m thick weakly developed palaeosol (2.9–2.45 m), whose parent material is brown (7.5YR 4/4) fine sand. The unit of 2.45–2.0 m is well developed dark-brown (10YR 4/3) palaeosol, with weak blocky structure. The uppermost unit (2.0–0 m) is well sorted yellowish-brown (10YR 6/4) aeolian sand. The bottom 0.4 m part of the uppermost unit has nearly horizontal bedding, while roots of modern vegetation can be found in the upper part without any bedding. Three OSL samples were collected at the transitional zone of sedimentary facies. Quartz grains from top of the bottom aeolian unit yielded an OSL age of 14.53±0.73 ka, and quartz grains from top of the dark palaeosol were OSL dated to 5.86±0.30 ka, while the OSL age of aeolian sand from bottom of the uppermost aeolian unit is 0.53±0.04 ka (Figure 3). palaeosol of this sequence began to develop at ca. 14.5 ka, and experienced remarkable pedogenesis in the middle Holocene. Although the OSL age from the bottom of the uppermost aeolian unit is about 0.53 ka, the real ending time of the palaeosol formation could not be determined due to the uncertainity of evaluation about potential erosions having occurred at the top of the palaeosol unit. It is, however, quite likely that the 2 m thick aeolian sand layer at top of the sequence was deposited during the past 500 years. There is a continuous litter layer around 0.8 m below the surface (Figure 3), which was deposited after AD 1950 according to its AMS ^{14}C age, indicating that the aeolian sands of the uppermost 0.8 m aeolian sand was deposited just in the last 60 years.

Overall, the entire section HLA consists in well sorted fine sands, although the palaeosol has significantly higher content of fine particles (<63 μm) and higher magnetic susceptibility (Figure 3). Field experiments showed that the increase of vegetation coverage in semi-arid areas could promote the ability to capture the atmospheric dust, which is the main provenance of fine particles in soils (Yan et al., 2011). Also, grain size analysis of aeolian sands collected from the surface with different vegetation coverage in the Maowusu Sandy Land indicated that the content of <63 μm particles increases significantly in fixed and semi-fixed dunes (Liu et al., 2017). Those observations and analyses suggest that the increasing content of fine particles in palaeosol should be closely related to the recovery of vegetation and stabilization

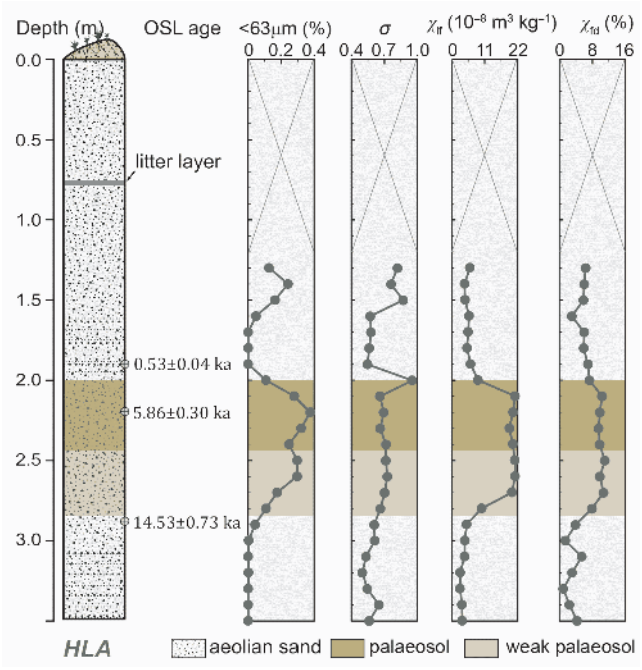

Figure 3 Stratigraphy, OSL chronology, and changes of palaeoenvironmental proxies in section HLA.

of dunes.

5. Discussion and conclusions

5.1 Age of the desert landscape and Holocene environmental changes deciphered from the sedimentary sequences of the Kubuqi Sand Sea

Although the oldest aeolian sand of the abovementioned 4 sections of the Kubuqi Sand Sea was OSL dated to ca. 16 ka (KD), we do not think it could be considered as direct evidence for the initiation of large-scale desert landscape in the Kubuqi, because the site of this sample is located near the river channel. Such a site is favorable for the formation of source-bordering dunes due to the availability of abundant loose sediments (Maroulis et al., 2007; Cohen et al., 2010; Halfen et al., 2016). Thus we assume that the aeolian deposition from the KD section mainly reflects the development of source-bordering dunes, and its formation should be closely linked to the fluvial sand supplies rather than climatic aridity. Just as Williams (1994) found, source-bordering dune development in western New South Wales of Australia was enhanced at times of warmer and wetter climate by replenishment of the localized fluvial-sand supply. Most of the sections studied by Fan et al. (2013) in the Kubuqi Sand Sea were dated to Holocene ages, broadly consistent with our results. However, the number of records is still too small for a full understanding of the origin and history of the Kubuqi Sand Sea. At this stage we are unable to clarify whether the aeolian depositional events in the interior of the Kubuqi reflect an increase of sand supply from the Yellow River (Liu and Yang, 2018) or the reworking of the underlying sandy sediments.

The OSL chronology of sections KA, KB, and KC indicates that the aeolian sands were deposited sometime in the last ~8 ka. As shown in Figure 2, the buried soils with cumulic A horizons could be found in both KA and KB, suggesting a vegetation rehabilitation and relative stable landscape for a prolonged period some times between ca. 4–2 ka. Generally speaking, the appearance of palaeosol in semi-arid regions reflects a steppe or forest-steppe landscape, while the appearance of aeolian sand corresponds to a desert landscape (Zhu et al., 1988; Yang and Eitel, 2016). In the KA and KB, the TOC and χ_{fd} of palaeosols are significantly higher than those of aeolian sands (Yang et al., 2016), indicating a relatively strong pedogenesis at that period. Consequently, we can infer that the Kubuqi Sand Sea might have had higher precipitation or effective moisture during 4–2 ka. The KC and KD sections in western parts of the Kubuqi Sand Sea do not have buried soils, indicating a continuous aridity. The modern environment monitoring of the Mauwusu Sandy Land, south of the Kubuqi Sand Sea, has shown that the responses to changes of external forcing between the western and eastern parts of the Maowusu Sandy Land are out-of-phase (Liang and Yang, 2016). The eastern part of the Mauwusu moved toward a better condition first under the trends of reduced wind power, weakened human intervention and a slight increase in precipitation, while the vegetation recovery in the western part is dependant more on a continuous improvement of climatic conditions (Liang and Yang, 2016). This study implies that there should be asynchronous responses to climate changes between the western and eastern parts of the Kubuqi Sand Sea due to the obviously different climate backgrounds.

As shown in Figure 2, the palaeosols were overlaid by aeolian sands, indicating enhanced aeolian activities in the Kubuqi Sand Sea 2000–1000 years ago. The timing of intensified aeolian activities is broadly consistent with the human expansion into this region during the Han (202 BC–AD 220) and Tang (AD 618–907) dynasties, reflecting their possible causal linkages. Research on historical geography as well as modern observations manifest that overgrazing and land reclamation can result in land degradation and dune reactivation in drylands (Zhu and Liu, 1981; Forman et al., 2008; Williams, 2014; Li and Yang, 2014; Liang and Yang, 2016; Cherlet et al., 2018). According to various historical literature, there were several population centers and county-level cities in the Kubuqi Sand Sea during the Neolithic and historical periods, respectively (Wang, 1991; Figure 4), and a large number of people had immigrated to the Kubuqi during the Qin and Han Dynasties. For example, the military of the Han Dynasty occupied the areas south of the Yellow River in 127 BC and they set up an administrative center named

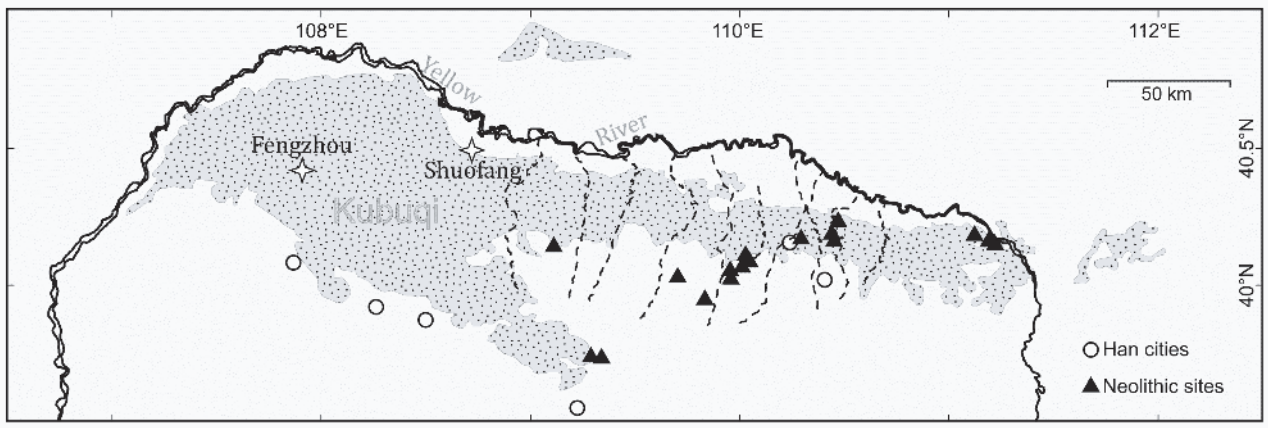

Figure 4 Distribution of Neolithic sites and Han cities (Chinese Cultural Bureau, 2003). Locations of the Fengzhou of the Tang Dynasty and Shuofang of the Han Dynasty are deciphered from Wang (1991).

"Shuofang" which governed over 10 counties (based on Ban Gu and Li Daoyuan, cited from Wang, 1991; Figure 4). The establishment of Shuofang spurred the economy in the northern frontier regions of the Chinese nation at that time.

Settlements may have existed in the Kubuqi Sand Sea as early as 3000 years ago, i.e., during Neolithic times (Figure 4). Driven by immigration policy for consolidating frontier defense after the Qin and Han Dynasties, a large number of people engaged in agricultural activities and diverted water for irrigation in the Kubuqi Sand Sea (Wang, 1991). The consumption of water from the Yellow River and its tributaries might have led to the desiccation of some parts of river beds, which would then provide additional loose sandy materials for the development of dunes (Liu and Yang, 2018), as it is commonly the case nowadays in western China (Yang et al., 2006a). Therefore, we conclude that the environmental deterioration of the Kubuqi Sand Sea in the late Holocene and the development of sand dunes was closely related to an intensification of human activities.

5.2 Holocene environmental changes of Hunshandake Sandy Land reflected by the aeolian-palaeosol sequences

Many shallow lake basins with remains of early shorelines exist in the Hunshandake Sandy Land, indicating significant variations of hydrological conditions. Typical lacustrine deposits were found at 1090 m above sea level in the western Hunshandake Sandy Land. Combining the analysis of digital elevation model, we think that the western Hunshandake might have been inundated under a single lake in the late Pleistocene (Yang et al., 2011). Although we failed to date these lacustrine deposits, it is likely that the initiation of the single lake would be earlier than 12–13 ka because of the ages of the lacustrine deposits at the bottom of the BN section (Figure 2). During the last deglaciation, the rivers springing from the southern mountains could have provided a large amount of water to form the great lake. We deduce that the appearance of the single lake was prior to the formation of dune landscape in the western Hunshandake Sandy Land. The viewpoint on the formation of the Hunshandake in the Pliocene claimed by Li and Dong (1998) needs further investigation. Periglacial sedimentary facies such as sand wedges found in the south of the Hunshandake indicate that continuous permafrost existed in northern China during the LGM and its southmost boundary could reach down to 38°N (Vandenberghe et al., 2004; Zhao et al., 2014), suggesting limited sediment availability for aeolian activities due to frozen conditions during the LGM.

The initial appearance of palaeosols in aeolian sequences can be interpreted as a sign of improved climatic conditions which resulted in the creation of stable landscapes and the suppression of aeolian processes. According to the OSL ages of the two sections, the initial soil formation of SX occurred later than that of BN (Figure 2). This offset could have been caused by the difference in the mean annual precipitation between the two sites (currently the precipitation difference between the west and east of Hunshandake is ca. 300 mm). We think that the post-Pleistocene climate change was time-transgressive across the region and that environment conditions had been improved slightly later at SX (west) than at BN (east). The bottom age of the palaeosol at the central-southern part of the Hunshandake is 9.36±0.27 ka (Yang et al., 2008), and broadly consistent with the result in the western part. Since the difference in ages is within the error bar of the OSL dating, the significant increase in moisture should be no later than 9 ka in the entire Hunshandake. In the eastern part of the Sandy Land, palaeo-drainage systems and high lake levels were dated to this time too (Yang et al., 2015; Goldsmith et al., 2017), indicating occurrence of a landscape with lakes, rivers and high vegetation coverage. Additionally, the radiocarbon age of a palaeo-spruce timber in the southern Hunshandake is 10040±100 yr BP (Cui et al., 1997), indicating a temperate humid forest from 10 to 9 ka in this region. Although the nature of OSL ages of our samples

cannot provide a high-resolution chronological framework for palaeoenvironmental reconstruction, we can conclude that the increase in effective moisture in the Hunshandake lasted at least from 9 ka to until around 3 ka. Combining the changes of palaeoenvironmental proxies and results from numerical simulations, Yang et al. (2013) suggested that there was likely an increase in mean annual precipitation of 30–140 mm during the early and middle Holocene in the Hunshandake. However, Zhou et al. (2008) demonstrated that the aeolian activities were still ongoing at 9.9–8.2 ka in the Hunshandake, and only gradually ceased during 8.2–2.7 ka.

The grain size variations in the BN section show that the palaeosol is finer than aeolian sand, but this trend is not significant in the SX section (Yang et al., 2013), confirming that the aeolian activities did not completely stop during the wetter periods. This is quite common in the semi-arid regions, i.e., as soil formation is in progress in one place, the aeolian deposition might be active nearby at the same time. While the vegetation grows, the dunes are being stabilized by vegetation and the organic matter gradually accumulates, forming a type of cumulic soil with an overthickened dark epipedon (Randall and Sharon, 2005).

5.3 Spatial and temporal variations of the aeolian activities in the dune fields in the eastern portion of the Chinese desert belt during the Holocene

Generally speaking, the extensive aeolian activities during the late Pleistocene have been reported for all sandy lands in the eastern part of the desert belt in northern China, with large-scale dune stabilization and soil development occurring in the middle Holocene (Figure 5), same as in the Hunshandake Sandy Land as discussed above. However, an even longer period of stabilization occurred during the early and middle Holocene in the dune fields located east of the Hunshandake, such as the Horqin Sandy and the Hulunbuir Sandy Land (Figures 3 and 5). Several aeolian sand-palaeosol sequences from the Horqin Sandy Land and their OSL ages showed that the dunes in the sandy land were stabilized during 7.5–2 ka and developed chernozem soil, and the period from 10 ka to 7.5 ka was characterized by the semi-stabilization of dunes in the Horqin (Zhao et al., 2007). The sections from later studies showed similar patterns (Yang et al., 2010, 2012), although the exact time of soil development is differently interpreted. The main features of the aeolian sedimentary sections in the Hulunbuir Sandy Land is a palaeosol interrupted by thin aeolian sands. Some previous studies demonstrated that the palaeosol of northern Hulunbuir has continued from 12.4 ka to 4.4 ka (Li and Sun, 2006) and even to a later date (Li et al., 2002). The aeolian sequence and OSL ages of the HLA section from the central Hulunbuir indicate that the environment had improved and a weak soil had begun to develop as early as 14.5 ka (Figure 3), while the strong soil formation only began at the middle Holocene and lasted until 2000 years ago (Figure 3). In the Maowusu Sandy Land, there was evidence showing that the period of aeolian activities was between 13 and 6 ka (Mason et al., 2009), and the time of soil development in the eastern Maowusu was between 7 and 2.4 ka (Lu et al., 2005), but some other records showed that the wetter period of the Maowusu was between 9 and 5.6 ka (Sun et al., 2006). Considering all previous studies, we think that the Hulunbuir Sandy Land experienced the longest period of stabilization among all the dune fields in the eastern portion of the desert belt of northern China (Figure 5). This must be linked with the relatively high mean annual precipitation and lower evapotranspiration associated with its geographic location at higher latitude and under lower temperatures (Figure 6).

It could be noted that the wetter period recorded by sedimentary sections at different sites varies more or less in the same dune field (Figure 5). Contradictory conclusions might be drawn from different sedimentary sections, showing the impact of spatial heterogeneity on the reconstruction of palaeoenvironment in arid and semiarid environments. This also illustrates the complexity of using the aeolian records to reconstruct the palaeoenvironment. For example, in contrast with our records at SX, BN and HLA sections, Mason et al. (2009) reported that dunes in the sandy lands of eastern China were still active during the earlier Holocene (11.5–8 ka). Even during the period between 8 and 6 ka, aeolian activities were not rare in these sandy lands (Mason et al., 2009). In order to reduce the impact of spatial heterogeneity and to construct a large-scale environmental change framework, Li and Yang (2016) used the published aeolian sand-palaeosol sequences and OSL chronological data to calculate the proportion of stable records in the INQUA dune chronological database. The results show that the palaeosol records in the dune fields of northern China account for more than 60% during the middle Holocene (Li and Yang, 2016; Figure 5), indicating that the sandy Lands in northern China should be in a stable state to a large extent during the Middle Holocene. However, OSL ages of the palaeosol have some uncertainties because the bioturbation is very common in the buried soil (Yang et al., 2013; Hesse, 2016). For reducing the uncertainties, we collect some OSL data following the criteria: (1) the data were published is peer-reviewed journals; (2) the stratigraphic features were clearly described; (3) the samples were collected from aeolian sand and no bioturbations were reported near the sampling points; (4) the OSL ages were reported with reliability evaluation and quality control. As of March 2018, a total of 135 aeolian event records matching the above four criterias have been published from the dune fields of eastern China (Figure 5). We used these collated OSL ages and their errors to calculate the cumulated probability density functions (Hesse, 2016;

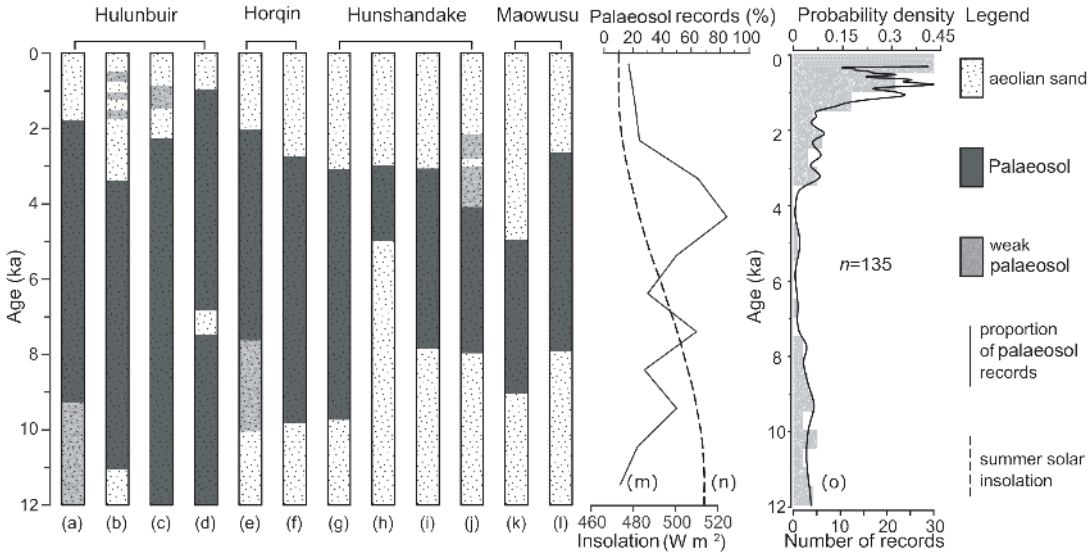

Figure 5 The typical Holocene aeolian sand-palaeosol sequences from the dune fields of eastern China ((a)–(l)), changes of solar insolation (June) at 30°N (n), the proportion of palaeosol records in the INQUA database (m), and the CPDF of aeolian sand OSL ages from the dune fields of eastern China (o). Origin of the data: (a), this study; (b), Li and Sun (2006); (c) Li et al. (2002); (d), Lu et al. (2013); (e) Zhao et al. (2007); (f) Yang et al. (2010); (g) this study; (h) Yang et al. (2008); (i) Mason et al. (2009); (j) Gong et al. (2013); (k) Sun et al. (2006); (l) Lu et al. (2005); (m) Li and Yang (2016); (n) Berger and Loutre (1991); (o) this study.

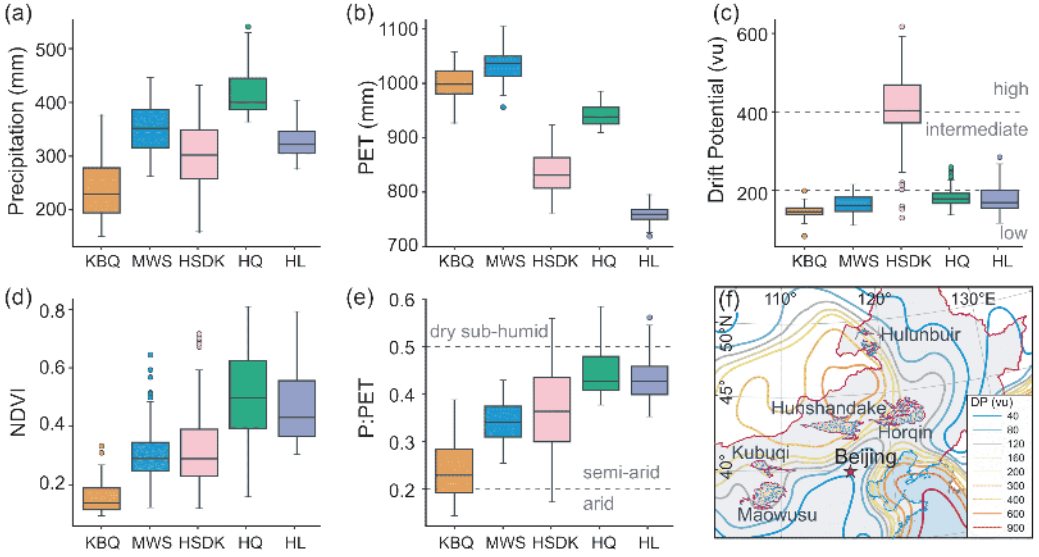

Figure 6 Comparison of modern climate and environment conditions in the dune fields of eastern China. (a) Mean annual precipitation (data from Fick and Hijmans, 2017); (b) mean annual Hargreaves potential evapotranspiration (data from Zomer et al., 2006); (c) Drift Potential (DP) of the wind from 1979 to 2017 (based on the ECWMF reanalysis data); (d) the MODIS NDVI of summer months; (e) the ratio of precipitation to potential evapotranspiration, degree of aridity based on UNEP (1997); (f) the random sampling sites (blue dots) distribution and DP isoline in north-eastern China. KBQ, Kubuqi; MWS, Maowusu; HSDK, Hunshandake; HQ, Horqin; HL, Hulunbuir.

Stauch, 2016), and the results show that the aeolian event records are mainly older than 7.5 ka or younger than 3.5 ka (Figure 5). This implies that the sandy lands in eastern China were extensively stabilized, and the aeolian processes were basically dormant during the period between 7.5 and 3.5 ka. The scattered aeolian depositional records in some sections are likely derived from some local aeolian events.

To understand the difference in responses to climate change in various dune fields, we conducted a random sampling analysis of the modern climate parameters of the dune fields in the eastern portion of the Chinese desert belt according to the extent of the sand areas (Figure 6). From the perspective of modern vegetation coverage reflected by the summer NDVI, the Horqin Sandy Land in the easternmost part and the Hulunbuir Sandy Land in the northernmost part show the highest NDVI (Figure 6d). The mean annual pre-

cipitation in each dune field varies generally from 200 to 500 mm (Figure 6a). And the Hunshandake Sandy Land has the largest regional difference in terms of mean annual rainfall (Figure 6a). Combining the potential evapotranspiration mainly associated with temperature (Zomer et al., 2006; Figure 6b), we calculated the effective moisture (mean annual precipitation/mean annual potential evapotranspiration, P/PET) of each dune field (Figure 6e). It comes out that there is a clear correlation between vegetation coverage and effective moisture (Figure 6d, e). The Kubuqi Sand Sea is the most arid one with an effective moisture <0.3, while the Hulunbuir Sandy Land and the Horqin Sandy Land are clearly wetter with an effective moisture >0.4 (Figure 6e). The wind power expressed by drift potential (DP, Fryberger and Dean, 1979) caculated using the wind data from 1979 to 2017 showed that the dune fields of our study belong to low wind energy environment with DP<200 vu except for the Hunshandake Sandy Land with a DP>200 vu (Figure 6c). The asynchrony of soil development and aeolian activities among different dune fields could be explained by the regional difference of climatic conditions in modern times. The better climatic conditions (i.e. with higher effective moisture) of the Hulunbuir and the Horqin Sandy Lands in the east enable them to respond more effectively to the improved climatic conditions in the early Holocene. However, the Maowusu and the Kubuqi in the west needed a higher and sustained increase in precipitation to have their dunes stabilized. This can be interpreted as time-transgressive processes on a larger scale than what was observed in the Hunshandake Sandy Land as reflected by the BN and SX sections. This also tells us that analyses of the modern climatic pattern are of great importances for palaeoenvironmental reconstructions.

5.4 Needs of studying the palaeoenvironment records and sedimentary sequences in the deserts of northern China and interpretational ambiguities requiring clarifications

In recent years, with the increasing amount of OSL ages derived from sedimentary sequences in deserts, ages of aeolian records themselves have become a proxy for interpreting the intensity of aeolian activities (Hesse, 2016; Stauch, 2016; Li and Yang, 2016). Driven by the international program 'The INQUA Dunes Atlas chronologic database' (Lancaster et al., 2016) the aeolian research community tries nowadays to investigate palaeoenvironmental changes in deserts and their responses to global climate change based on a convincing number of sedimentary records/sections rather than using a single section as earlier (Lancaster et al., 2016; Thomas and Bailey, 2017). In light of the standard of the INQUA Dunes Atlas chronologic database, Li and Yang (2016) collated data from published literature, and 331 dune records from the dune fields of northern China have been compiled in the INQUA database. Most of these ages from China were OSL dated, while only 25 were dated by radiocarbon methods. There are obviously spatial and temporal imbalance in terms of the record availability in the sand seas and sandy lands of northern China in the current database. From the perspective of temporal range, most of the records are within the time since the LGM, of which about 85% are from the Holocene (Li and Yang, 2016). Compared to other areas, the arid and semi-arid regions often experience strong aeolian erosion and rapid reworking processes. Therefore, the aeolian depositions are difficult to be fully preserved over long geological history. This could lead to the decrease in the number of aeolian depositional records with increasing ages (Li and Yang, 2016). In terms spatial coverage, the number of records is obviously higher in the dune fields of the eastern portion of the Chinese desert belt than that in the west. Only sporadic records have been published about the Taklamakan Sand Sea, the largest dune field in northern China. Although much more age data about the sandy lands in the east can be found, most of these records are younger than 20 ka, potentially due to sand availability and preservation (Li and Yang, 2016). Even so, the number of available palaeoenvironmental records in the sandy lands of eastern China is still far from satisfactory to depict precisely the history of the environmental changes in this part of the world. In the INQUA Dunes Atlas chronologic database published in 2016, there were over 600 age records from both the dune fields of South Africa and Australia, and those from the dune fields of North America reached up to 1000 (Lancaster et al., 2016; Hesse, 2016; Halfen et al., 2016), showing that there is still a large gap between China and other countries in the study of palaeoenvironments of deserts.

In arid and semi-arid areas where palaeoenvironmental archives are rare, aeolian deposits play a unique role in the reconstruction of past climate changes. However, the following ambiguities are often difficult to be clarified although they are crucial to the interpretation of the palaeoenvironmental records in these regions:

(1) Spatial heterogeneity is a common fact in the dune fields of northern China (especially in the sandy lands). In a same area, the nature of earth surface between dunes and inter-dunes can be different and active dunes and semi-stabilized dunes often coexist. Even on a same dune, the vegetation coverage on the stoss side and the lee could be quite different. This alone would lead to inconsistent sequences because of selection of micro morphology. When reconstructing the palaeoenvironments of the desert, it is necessary to obtain as many sediment records as possible to clarify and avoid the potential impacts of spatial heterogeneity.

(2) Sampling location for chronological samples affects

the interpretation of the palaeoenvironments. Practically, the OSL method is well-suited and easily applied for handling aeolian sediments (Rhodes, 2011), thus most of the OSL samples are collected from aeolian sand units in an aeolian sand-palaeosol/lacustrine sedimentary sequence, while OSL samples from palaeosol/lacustrine units are sometimes avoided. Therefore, only considering the number of age records would lead to overestimating/underestimating the dune activity/stability. In addition, new phase of aeolian activities might be just a reworking of previously deposited sediments from an existing dune system (Kocurek, 1998), resulting in a lower probability of preserving older deposits, and thus sample ages could be concentrated in more recent periods (Figure 5). Provided older deposits would still be preserved in lower layers, the sampling strategy may cause samples to tend to be young (Thomas and Bailey, 2017). Therefore, the significant increase of age records for the last 2000 years does not necessarily mean that the aeolian activities were stronger in that period than those in the early Holocene.

(3) The relationship between the intensity of aeolian activity and climatic conditions is quite complex. In the early studies, the appearance of palaeosol was mostly interpreted as a sign of climate optimum, vegetation development and desert contraction, while the appearance of aeolian sands was associated with drier climate, increase in aeolian activities and desert expansion (e.g., Thomas et al., 2005; Mason et al., 2009; Yang and Eitel, 2016). However, studies from the Gonghe Basin in the Qinghai-Tibetan Plateau indicated that the appearance of aeolian landscapes is mainly subject to changes in sediment supply, and there is no straightforward relationship between aeolian activities and climate conditions (Qiang et al., 2016). Muhs and Holliday (2001) found out that the regional dune stabilization in the southern high plains of the United States in the late Holocene is firstly related to the reduction in sediment availability, and then to the change of precipitation. Studies from the Hunshandake Sandy Land showed that the direct trigger for an irreversible and abrupt desertification were the changes in its hydrology caused by headward erosion and groundwater sapping (Yang et al., 2015). The movement of dunes in South Africa cannot be completely explained by the simple linear relationship of "shifting of sand dunes-aridification enhancement", either (Chase, 2009). These studies challenged the previous theories applying dune activity as an indicator of climate aridification and demonstrated that it is important to understand geomorphology and surface process prior to reconstructing palaeoenvironments in desert.

Unlike other relatively continuous palaeoclimate records such as loess deposits and stalagmites, aeolian sand deposits are characterized by typical intermittency and instantaneity (Zhang and Yang, 2016). Although the occurrence of aeolian sand accumulation could reflect the history of aeolian activities, erosion of sedimentary records is an important part of geomorphological processes in aeolian systems (Williams, 2014; Thomas and Bailey, 2017). Thus, method establishing high-resolution framework of environmental changes from ages of aeolian sands and tuning these changes with other high-resolution climate records to depict the responses of desert environment to centennial/decadal climate fluctuations require reassessments.

Acknowledgements *Sincere thanks are extended to Academician GUO Zhengtang and the staffs of the project office for their much-appreciated help and supervisions. We also thank two anonymous reviewers for their valuable comments on earlier drafts of this manuscript. We authors would like to dedicate the work to Academician SUN Shu, a giant of Earth Sciences, who sadly passed away while we wrote this article. We deeply cherish our memory of the great mentor. This work was supported by the CAS Strategic Priority Research Program (Grant No. XDA05120502) and the National Natural Science Foundation of China (Grant No. 41672182).*

References

Berger A, Loutre M F. 1991. Insolation values for the climate of the last 10 million years. Quat Sci Rev, 10: 297–317
Chase B. 2009. Evaluating the use of dune sediments as a proxy for palaeoaridity: A southern African case study. Earth-Sci Rev, 93: 31–45
Chen F, Wu W, Zhu Y, Holmes J A, Madsen D B, Jin M, Oviatt C G. 2003. A mid-Holocene drought interval as evidenced by lake desiccation in the Alashan Plateau, Inner Mongolia, China. Chin Sci Bull, 48: 1401–1410
Cherlet M, Hutchinson C, Reynolds J, Hill J, Sommer S, von Maltitz G. 2018. World Atlas of Desertification. 3rd ed. Luxembourg: Publication Office of the European Union
Chinese Cultural Bureau. 2003. The Atlas of Chinese Cultural Sites: Inner Mongolia (in Chinese). Xi'an: Xi'an Cartographic Publishing House
Cohen T J, Nanson G C, Larsen J R, Jones B G, Price D M, Coleman M, Pietsch T J. 2010. Late Quaternary aeolian and fluvial interactions on the Cooper Creek Fan and the association between linear and source-bordering dunes, Strzelecki Desert, Australia. Quat Sci Rev, 29: 455–471
Cui H, Liu H, Yao X. 1997. The finding of a palaeo-spruce timber in Hunshandak sandy land and its palaeoecological significance. Sci China Ser D-Earth Sci, 40: 599–604
Dai A. 2013. Increasing drought under global warming in observations and models. Nat Clim Change, 3: 52–58
Evans R D, Koyama A, Sonderegger D L, Charlet T N, Newingham B A, Fenstermaker L F, Harlow B, Jin V L, Ogle K, Smith S D, Nowak R S. 2014. Greater ecosystem carbon in the Mojave Desert after ten years exposure to elevated CO_2. Nat Clim Change, 4: 394–397
Fan Y X, Chen X L, Fan T L, Jin M, Liu J B, Chen F H. 2013. Sedimentary and OSL dating evidence for the development of the present Hobq desert landscape, northern China. Sci China Earth Sci, 56: 2037–2044
Fick S E, Hijmans R J. 2017. WorldClim 2: New 1-km spatial resolution climate surfaces for global land areas. Int J Climatol, 37: 4302–4315
Folk R L, Ward W C. 1957. Brazos River bar: A study in the significance of grain size parameters. J Sediment Res, 27: 3–26
Forman S L, Sagintayev Z, Sultan M, Smith S, Becker R, Kendall M, Marìn L. 2008. The twentieth-century migration of parabolic dunes and wetland formation at Cape Cod National Sea Shore, Massachusetts, USA: Landscape response to a legacy of environmental disturbance. Holocene, 18: 765–774
Fryberger S, Dean G. 1979. Dune forms and wind regime. In: McKee E, ed. A Study of Global Sand Seas, Washington: United States Geological Survey Professional Paper 1052. 137–169
Gong Z, Li S H, Sun J, Xue L. 2013. Environmental changes in Hunshandake (Otindag) sandy land revealed by optical dating and multi-

proxy study of dune sands. J Asian Earth Sci, 76: 30–36
Goudie A. 2002. Great Warm Deserts of the World: Landscapes and Evolution. New York: Oxford University Press
Guérin G, Mercier N, Adamiec G. 2011. Dose-rate conversion factors: Update. Ancient TL, 29: 5–8
Guo L, Xiong S, Yang P, Ye W, Jin G, Wu W, Zhao H. 2018. Holocene environmental changes in the Horqin desert revealed by OSL dating and $\delta^{13}C$ analyses of palaeosols. Quat Int, 469: 11–19
Guo Z, Ren X, Lv H, Gao X, Liu W, Wu H, Zhang C, Zhang J. 2016. Effect of palaeoclimate changes and human adaptation—Progress on "Impact and Adaptation" group of CAS strategic priority research program "climate change: Carbon budget and relevant issues" (in Chinese with English abstract). Bull Chin Acad Sci, 31: 142–151
Halfen A F, Lancaster N, Wolfe S. 2016. Interpretations and common challenges of aeolian records from North American dune fields. Quat Int, 410: 75–95
Heller F, Liu X, Liu T, Xu T. 1991. Magnetic susceptibility of loess in China. Earth Planet Sci Lett, 103: 301–310
Hesse P P. 2016. How do longitudinal dunes respond to climate forcing? Insights from 25 years of luminescence dating of the Australian desert dunefields. Quat Int, 410: 11–29
Huang J, Yu H, Guan X, Wang G, Guo R. 2016. Accelerated dryland expansion under climate change. Nat Clim Change, 6: 166–171
IPCC. 2013. Climate Change 2013—The Physical Science Basis: Working Group I Contribution to the Fifth Assessment Report of the IPCC. Cambridge: Cambridge University Press
Kocurek G. 1998. Aeolian system response to external forcing factors—A sequence stratigraphic view of the Saharan region. In: Alsharan S, Glennie W, Whittle L, Kendall C, eds. Quaternary Deserts and Climatic Change. Rotterdam: A.A. Balkema. 327–337
Lancaster N, Yang X, Thomas D. 2013. Spatial and temporal complexity in Quaternary desert datasets: Implications for interpreting past dryland dynamics and understanding potential future changes. Quat Sci Rev, 78: 301–302
Lancaster N, Wolfe S, Thomas D, Bristow C, Bubenzer O, Burrough S, Duller G, Halfen A, Hesse P, Roskin J, Singhvi A, Tsoar H, Tripaldi A, Yang X, Zárate M. 2016. The INQUA Dunes Atlas chronologic database. Quat Int, 410: 3–10
Li S H, Sun J M, Zhao H. 2002. Optical dating of dune sands in the northeastern deserts of China. Palaeogeogr Palaeoclimatol Palaeoecol, 181: 419–429
Li S H, Sun J. 2006. Optical dating of Holocene dune sands from the Hulun Buir Desert, northeastern China. Holocene, 16: 457–462
Li H, Yang X. 2014. Temperate dryland vegetation changes under a warming climate and strong human intervention—With a particular reference to the district Xilin Gol, Inner Mongolia, China. Catena, 119: 9–20
Li H, Yang X. 2016. Spatial and temporal patterns of aeolian activities in the desert belt of northern China revealed by dune chronologies. Quat Int, 410: 58–68
Li X, Dong G. 1998. Preliminary studies on the age and formation of the Hunshandake Sandy Land (in Chinese with English abstract). J Desert Res, 18: 16–21
Li Y, Wang Y G, Houghton R A, Tang L S. 2015. Hidden carbon sink beneath desert. Geophys Res Lett, 42: 5880–5887
Liang P, Yang X. 2016. Landscape spatial patterns in the Maowusu (Mu Us) Sandy Land, northern China and their impact factors. Catena, 145: 321–333
Liu B, Jin H, Sun L, Sun Z, Zhang C. 2017. Grain size and geochemical study of the surface deposits of the sand dunes in the Mu Us desert, northern China. Geol J, 52: 1009–1019
Liu J, Fa K, Zhang Y, Wu B, Qin S, Jia X. 2015. Abiotic CO_2 uptake from the atmosphere by semiarid desert soil and its partitioning into soil phases. Geophys Res Lett, 42: 5779–5785
Liu Q, Yang X. 2018. Geochemical composition and provenance of aeolian sands in the Ordos Deserts, northern China. Geomorphology, 318: 354–374
Lu H, Miao X, Zhou Y, Mason J, Swinehart J, Zhang J, Zhou L, Yi S. 2005. Late Quaternary aeolian activity in the Mu Us and Otindag dune fields (north China) and lagged response to insolation forcing. Geophys Res Lett, 32: L21716
Lu H Y, Yi S W, Xu Z W, Zhou Y L, Zeng L, Zhu F Y, Feng H, Dong L N, Zhuo H X, Yu K F, Mason J, Wang X Y, Chen Y Y, Lu Q, Wu B, Dong Z B, Qu J J, Wang X M, Guo Z T. 2013. Chinese deserts and sand fields in Last Glacial Maximum and Holocene optimum. Chin Sci Bull, 58: 2775–2783
Maroulis J C, Nanson G C, Price D M, Pietsch T. 2007. Aeolian-fluvial interaction and climate change: Source-bordering dune development over the past ~100 ka on Cooper Creek, central Australia. Quat Sci Rev, 26: 386–404
Mason J A, Lu H, Zhou Y, Miao X, Swinehart J B, Liu Z, Goble R J, Yi S. 2009. Dune mobility and aridity at the desert margin of northern China at a time of peak monsoon strength. Geology, 37: 947–950
Muhs D R, Holliday V T. 2001. Origin of late Quaternary dune fields on the Southern High Plains of Texas and New Mexico. Geol Soc Am Bull, 113: 75–87
Murray A S, Wintle A G. 2000. Luminescence dating of quartz using an improved single-aliquot regenerative-dose protocol. Radiat Meas, 32: 57–73
Murray A S, Wintle A G. 2003. The single aliquot regenerative dose protocol: Potential for improvements in reliability. Radiat Meas, 37: 377–381
Pye K, Tsoar H. 2009. Aeolian Sand and Sand Dunes. Berlin: Springer
Qiang M, Jin Y, Liu X, Song L, Li H, Li F, Chen F. 2016. Late Pleistocene and Holocene aeolian sedimentation in Gonghe Basin, northeastern Qinghai-Tibetan Plateau: Variability, processes, and climatic implications. Quat Sci Rev, 132: 57–73
Randall JS, Sharon A. 2005. Soils: Genesis and Geomorphology. New York: Cambridge University Press
Rhodes E J. 2011. Optically stimulated luminescence dating of sediments over the past 200000 years. Annu Rev Earth Planet Sci, 39: 461–488
Stauch G. 2016. Multi-decadal periods of enhanced aeolian activity on the north-eastern Tibet Plateau during the last 2 ka. Quat Sci Rev, 149: 91–101
Stauch G, IJmker J, Pötsch S, Zhao H, Hilgers A, Diekmann B, Dietze E, Hartmann K, Opitz S, Wünnemann B, Lehmkuhl F. 2012. Aeolian sediments on the north-eastern Tibetan Plateau. Quat Sci Rev, 57: 71–84
Stone R. 2008. Have desert researchers discovered a hidden loop in the carbon cycle? Science, 320: 1409–1410
Sun J, Li S H, Han P, Chen Y. 2006. Holocene environmental changes in the central Inner Mongolia, based on single-aliquot-quartz optical dating and multi-proxy study of dune sands. Palaeogeogr Palaeoclimatol Palaeoecol, 233: 51–62
Thomas D S G, Bailey R M. 2017. Is there evidence for global-scale forcing of Southern Hemisphere Quaternary desert dune accumulation? A quantitative method for testing hypotheses of dune system development. Earth Surf Process Landforms, 42: 2280–2294
Thomas D S G, Knight M, Wiggs G F S. 2005. Remobilization of southern African desert dune systems by twenty-first century global warming. Nature, 435: 1218–1221
UNEP (United Nations Environment Programme). 1997. World Atlas of Desertification. 2nd ed. London: UNEP
Vandenberghe J, Zhijiu C, Liang Z, Wei Z. 2004. Thermal-contraction-crack networks as evidence for late-Pleistocene permafrost in Inner Mongolia, China. Permafrost Periglac Process, 15: 21–29
Wang B. 1991. Historical geography study of the Kubuqi Desert (in Chinese). J Desert Res, 11: 33–41
Williams M. 1994. Some implications of past climatic changes in Australia. T Roy Soc South Aust, 118: 17–25
Williams M. 2014. Climate Change in Deserts: Past, Present and Future. New York: Cambridge University Press
Wohlfahrt G, Fenstermaker L F, Arnone III J A. 2008. Large annual net ecosystem CO_2 uptake of a Mojave Desert ecosystem. Glob Change

Biol, 14: 1475–1487
Yan Y, Xu X, Xin X, Yang G, Wang X, Yan R, Chen B. 2011. Effect of vegetation coverage on aeolian dust accumulation in a semiarid steppe of northern China. Catena, 87: 351–356
Yang L H, Zhou J, Lai Z P, Long H, Zhang J R. 2010. Lateglacial and Holocene dune evolution in the Horqin dunefield of northeastern China based on luminescence dating. Palaeogeogr Palaeoclimatol Palaeoecol, 296: 44–51
Yang L H, Wang T, Zhou J, Lai Z P, Long H. 2012. OSL chronology and possible forcing mechanisms of dune evolution in the Horqin dunefield in northern China since the Last Glacial Maximum. Quat Res, 78: 185–196
Yang L H, Wang T, Long H, He Z. 2017. Late Holocene dune mobilization in the Horqin dunefield of northern China. J Asian Earth Sci, 138: 136–147
Yang X. 2000. Landscape evolution and precipitation changes in the Badain Jaran Desert during the last 30000 years. Chin Sci Bull, 45: 1042–1047
Yang X, Eitel B. 2016. Understanding the interactions between climate change, landscape evolution, surface processes and tectonics in the earth system: What can the studies of Chinese deserts contribute? Acta Geol Sin-Engl Ed, 90: 1444–1454
Yang X, Liu T, Xiao H. 2003. Evolution of megadunes and lakes in the Badain Jaran Desert, Inner Mongolia, China during the last 31,000 years. Quat Int, 104: 99–112
Yang X P, Preusser F, Radtke U. 2006. Late Quaternary environmental changes in the Taklamakan Desert, western China, inferred from OSL-dated lacustrine and aeolian deposits. Quat Sci Rev, 25: 923–932
Yang X, Dong J, White P D. 2006a. The key role of water resources management in ecological restoration in western China. Geogr Res, 44: 146–154
Yang X, Zhu B, Wang X, Li C, Zhou Z, Chen J, Wang X, Yin J, Lu Y. 2008. Late Quaternary environmental changes and organic carbon density in the Hunshandake Sandy Land, eastern Inner Mongolia, China. Glob Planet Change, 61: 70–78
Yang X, Scuderi L, Paillou P, Liu Z, Li H, Ren X. 2011. Quaternary environmental changes in the drylands of China—A critical review. Quat Sci Rev, 30: 3219–3233
Yang X P, Wang X L, Liu Z T, Li H W, Ren X Z, Zhang D G, Ma Z B, Rioual P, Jin X D, Scuderi L. 2013. Initiation and variation of the dune fields in semi-arid China-with a special reference to the Hunshandake Sandy Land, Inner Mongolia. Quat Sci Rev, 78: 369–380
Yang X P, Scuderi L A, Wang X L, Scuderi L J, Zhang D G, Li H W, Forman S, Xu Q H, Wang R C, Huang W W, Yang S X. 2015. Groundwater sapping as the cause of irreversible desertification of Hunshandake Sandy Lands, Inner Mongolia, northern China. Proc Natl Acad Sci USA, 112: 702–706
Yang X P, Forman S, Hu F G, Zhang D G, Liu Z T, Li H W. 2016. Initial insights into the age and origin of the Kubuqi sand sea of northern China. Geomorphology, 259: 30–39
Zhao H, Yanchou Lu H, Yin J. 2007. Optical dating of Holocene sand dune activities in the Horqin sand-fields in inner Mongolia, China, using the SAR protocol. Quat Geochronol, 2: 29–33
Zhao L, Jin H, Li C, Cui Z, Chang X, Marchenko S S, Vandenberghe J, Zhang T, Luo D, Guo D, Liu G, Yi C. 2014. The extent of permafrost in China during the local Last Glacial Maximum (LLGM). Boreas, 43: 688–698
Zhang D, Yang X. 2016. Numerical simulation on sand dune morphodynamic: A case study of ReSCAL model (in Chinese with English Abstract). Quat Sci, 37: 368–379
Zhang H, Ma Y, Peng J, Li J, Cao J, Qi Y, Chen G, Fang H, Mu D, Pachur H J, Wünnemann B, Feng Z. 2002. Palaeolake and palaeoenvironment between 42 and 18 ka BP in Tengger Desert, NW China. Chin Sci Bull, 47: 1946–1956
Zhou Y L, Lu H Y, Joseph M, Miao X D, James S, Ronald G. 2008. Optically stimulated luminescence dating of aeolian sand in the Otindag dune field and Holocene climate change. Sci China Ser D-Earth Sci, 51: 837–847
Zhu Z, Wu Z, Liu S, Di X. 1980. An Outline of Chinese Deserts (in Chinese). Beijing: Science Press
Zhu Z, Liu S. 1981. Desertification Processes and their Control in Northern China (in Chinese). Beijing: China Forestry Press
Zhu Z, Zou B, Di X, Wang K, Chen G, Zhang J. 1988. Desertification and rehabilitation-Case study in Horqin Sandy Land. Lanzhou: Institute of Desert Research, Chinese Academy of Sciences. 113
Zomer R, Trabucco A, van Straaten O, Bossio D. 2006. Carbon, land and water: A global analysis of the hydrologic dimensions of climate change mitigation through afforestation/reforestation. Colombo, Sri Lanka: International Water Management Institute. 44

(Responsible editor: Huayu LU)